Academic Journal of Science and Technology
ISSN: 2771-3032 | Vol. 10, No. 1, 2024

Simulation Analysis of Single-tooth Rock Breaking Process

Yang Chun, Bin Li

School of Mechanical and Electrical Engineering, Southwest Petroleum University, Chengdu, 610500, China

Abstract: In this paper, the rock breaking process of the cutting teeth is analyzed, firstly, based on the rock constitutive model and damage law, the simulation model is established by finite element software, and the cutting load of the cutting teeth in the plane rock, rock ridge and rock ridge root is analyzed, and on this basis, the load of the rock and the cutting tooth during scraping is analyzed through the cloud map. The effects of camber angle, depth and cutting speed on cutting force and crushing ratio were analyzed.

Keywords: Rock breaking, PDC cutting teeth, Abaqus.

1. Rock Constitutive Model and Rock Damage Law

1.1. Rock constitutive relations

In the stage of elastic deformation of rock under load, generalized Hooke's law can be used to solve the rock strain problem in plane and space.

In the plane problem, the constitutive relation of the rock is given by the following expression[1]:

$$\begin{cases} \varepsilon_x = \dfrac{1-v^2}{E}\left[\sigma_x - \sigma_y \dfrac{v}{1-v}\right] \\ \varepsilon_y = \dfrac{1-v^2}{E}\left[\sigma_y - \sigma_x \dfrac{v}{1-v}\right] \\ \gamma_{xy} = \dfrac{2}{E}(1+v)\tau_{xy} \end{cases} \tag{1}$$

For space problems, the constitutive equation for a rock is as follows

$$\begin{cases} \varepsilon_x = \dfrac{1}{E}\left[\sigma_x - \upsilon(\sigma_y + \sigma_z)\right] \\ \varepsilon_y = \dfrac{1}{E}\left[\sigma_y - \upsilon(\sigma_x + \sigma_z)\right] \\ \varepsilon_y = \dfrac{1}{E}\left[\sigma_z - \upsilon(\sigma_x + \sigma_y)\right] \\ \gamma_{yz} = \dfrac{2(1+\upsilon)}{E}\tau_{yz} \\ \gamma_{zx} = \dfrac{2(1+\upsilon)}{E}\tau_{zx} \\ \gamma_{xy} = \dfrac{2(1+\upsilon)}{E}\tau_{xy} \end{cases} \tag{2}$$

In the plastic deformation stage of rock, three sets of equations are required to describe its plastic deformation, which express the rock yield condition, the loading and unloading criterion and the constitutive equation respectively.

During the plastic deformation of rocks, the size and shape of the yield surface change, and can be divided into three yield models according to their characteristics: isotropic hardening-softening model, follow-up hardening model, and hybrid hardening model. The commonly used yield criterion is divided into "Coulomb criterion", "Mohr strength theory", "Griffith strength theory" and "Drucker-Prager" criterion, i.e., D-P criterion.

1.2. Rock yield criterion

Different yield criteria have different objects and conditions, and the yield criterion is also the basis for rock failure judgment.

(1) Coulomb criterion

This criterion is known as the shear strength criterion for planar problems, and the expression[2]:

$$|\tau| = c + \sigma \tan\phi \tag{3}$$

τ -shear strength;

σ -normal stress;

φ -Angle of friction within the rock;

c -Adhesion.

The diagram of the Coulomb criterion is shown in Figure 1-1 below, when the stress circle is secant to the equation line, that is, the point on the circle falls outside the equation oblique line, it indicates that the stress at the point has exceeded the material strength of the rock, and the rock will be destroyed. Conversely, if it falls within the slash of the equation, the rock will not be destroyed; If the point falls within the slash of the equation, it will not be destroyed; If the stress circle is tangent to the straight line, i.e., the point falls above the tangent of the equation, then the rock is in a critical state.

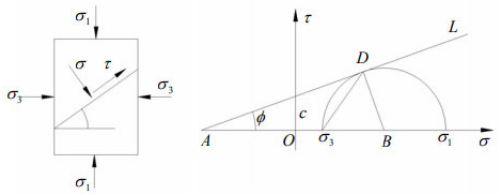

Figure 1-1. Coulomb criterion Diagram

The Coulomb criterion uses the expression of the maximum shear stress and the average stress[3]:

$$\tau_m = \sigma_m \sin\phi + c\cos\phi \tag{4}$$

$\tau_m = \frac{1}{2}(\sigma_1 - \sigma_3)$ is the maximum shear stress;

$\sigma_m = \frac{1}{2}(\sigma_1 + \sigma_3)$ is the average principal stress.

The Coulomb criterion uses expressions for principal stresses, rock fracture angles, and uniaxial compressive strength of rocks

$$\sigma_1 = \sigma_3 \tan^2\theta + \sigma_c \tag{5}$$

where: is the angle of rock breakage, and the relationship with the angle of friction of the rock is

$$2\theta = \frac{\pi}{2} + \phi \tag{6}$$

Based on the transformation and discussion of the equation and the analysis of the experimental results, four rock breaking methods based on the simplified equation and the equation are given:

$$\begin{cases} \sigma_1\left[\sqrt{f^2+1}-f\right]-\sigma_3\left[\sqrt{f^2+1}+f\right]=2c & (\sigma_1 > \frac{1}{2}\sigma_c) \\ \sigma_3 = -\sigma_1 & (\sigma_1 \le \frac{1}{2}\sigma_c) \end{cases} \tag{7}$$

where $\tan\phi = f$

Rock breaking methods and conditions

1. Uniaxial tensile breakage

$$0 \le \sigma_1 \le \frac{1}{2}\sigma_c (\sigma_3 = -\sigma_1) \tag{8}$$

2. Biaxial tensile failure

$$\frac{1}{2}\sigma_c \le \sigma_1 \le \sigma_c (-\sigma_1 < \sigma_3 < 0) \tag{9}$$

3.Uniaxial compression failure

$$\sigma_1 = \sigma_c (\sigma_3 = 0) \tag{10}$$

4. Biaxial compression breakage

$$\sigma_1 > \sigma_c (\sigma_3 > 0) \tag{11}$$

(1) Mohr's strength theory [4]

In1900, on the basis of the Coulomb criterion, Mohr generalized from the plane problem to the three-way stress state. He proposed that "when a material reaches its limit, the shear stress on the sliding plane reaches a maximum value depending on the normal stress and the properties of the material", which can be expressed as a function as follows

$$\tau = f(\sigma) \tag{12}$$

Compared with the single linear envelope of the Coulomb criterion, the Mohr strength theory adds three envelope types: oblique straight line, quadratic parabolic and hyperbola, which broadens the scope of application to meet the needs of the model in different situations, analyzes the characteristics of the two criteria before and after, and can also take the linear type in the Coulomb criterion as a special case in the Mohr criterion. In general, the strength envelope of weaker rocks such as marl, sandstone, and shale is similar to that of a quadratic parabola, and its shape expression is shown in Figure 1-2 below

$$\tau^2 = n(\sigma + \sigma_t) \tag{13}$$

where — uniaxial tensile strength of rock

From Figure 1-2, the relationship between the principal stress, shear stress and other parameters can be deduced:

$$\begin{cases} \frac{1}{2}(\sigma_1 + \sigma_3) = \sigma + \tau\cot 2\alpha \\ \frac{1}{2}(\sigma_1 - \sigma_3) = \frac{\tau}{\sin 2\alpha} \end{cases} \tag{14}$$

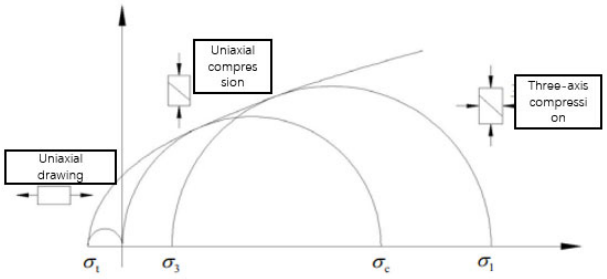

Figure 1-2. Strength Envelope Line of Rock

(1) Drucker-Pragley Theory (D-P Theory)[5]

Drucker and Prager took hydrostatic stress into account in the middle of the last century, and because of the consideration of intermediate principal stress, it is theoretically closer to the actual situation of engineering practice, and even though later generations have continuously corrected and supplemented it more perfectly, it is still widely used until now.

$$\begin{cases} \sigma_1 = \sigma_c + a\sigma_3^b \\ \tau_{13}^n = \sigma_c + a\sigma_3^b \\ \tau_{13} = \sigma_c + a\sigma_{13} \end{cases} \tag{15}$$

In this paper, the linear D-P criterion is taken as the research object. The yield function expression for the linear D-P criterion is:

$$f = t - p\tan\beta - d = 0 \tag{16}$$

where $t = \frac{1}{2}q\left[1 + \frac{1}{k} - \left(1 - \frac{1}{k}\right)\left(\frac{r}{q}\right)^3\right]$ is the shear

stress on the shear surface.

In order to simplify the research content, this paper takes the special form of the M-C criterion, the linear M-C criterion, as the research object, and introduces this correspondence. The yield surface formed by the linear M-C criterion is represented in the stress space of σ1, σ2, and σ3 as a sharp hexagonal pyramid. The graph represented by the yield surface in the spatial structure is shown in Figure 1-3.

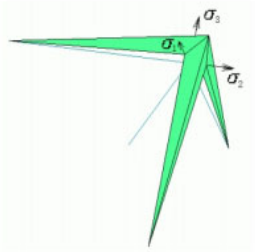

Figure 1-3. Yield surface structure expressed in space by linear M-C criterion

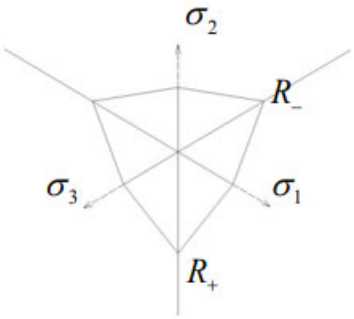

Figure 1-4. Hexagonal port surface cut from the plane

A hexagonal port cut is obtained by cutting the yield surface with a π plane (the hydrostatic pressure axis σ1=σ2=σ3 is the face in the normal direction), as shown in Figure 1-4. From the figure, we can find that the obtained two positive and negative intercepts (R+, R-) correspond to the positive and negative intercept line segments passing through the top of the hexagonal pyramid. There are 6 sharp corners in this cross-section, and when the associated plastic flow law is used, the direction of the plastic flow will be different, and the calculation will be difficult or even non-convergent when using finite element calculations.

The D-P criterion transforms the hexagonal pyramidal structure in the stress space of the M-C criterion into a regular conic structure, as shown in Figure 1-5. After π plane cut, a circular port cut is obtained, as shown in Figure 4-6, which avoids the problem of instability and non-convergence caused by sharp corners. The radius of the circular port cut is determined by the position of the π plane.

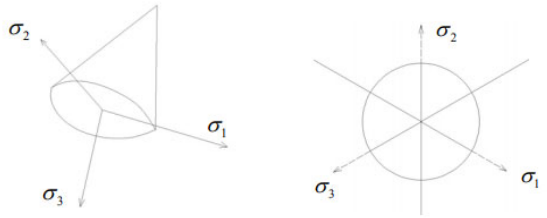

Figure 1-5. Yield structure expressed by linear D-P criterion in space Figure 1-6 Circular port surface cut by plane

The D-P criterion is based on the M-C criterion, and adopts the gradual approximation method to avoid the appearance of sharp corners on the π plane. Figure 1-7 When the D-P criterion is based on R-, the yield surface of the rock on the π plane is obtained. Fig. 1-8 When the D-P criterion is based on R+, the yield surface of the rock on the π plane is obtained.

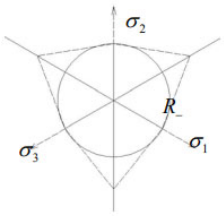

Figure 1-7. Negative intercept approximation

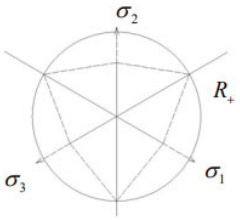

Figure 1-8. Positive intercept approximation

According to the negative intercept approximation, the yield surface of the rock is smaller, and according to this method, the rock is too conservative in theoretical calculation, which can not maximize the characteristics of the rock and increase the project cost. If the approximation is based on the positive intercept, the results obtained in theoretical calculations will be dangerous. Therefore, neither of these approximation methods alone is reasonable.

The approximation method is controlled by setting the ratio of tensile to compressive strength of the rock K, which is limited to 0.778 and 1 in the actual finite element simulation to ensure that the calculation is correct. When the K value changes in this range, the yield surface of the rock on the π plane (bias plane) is obtained as shown in Figure 1-9.

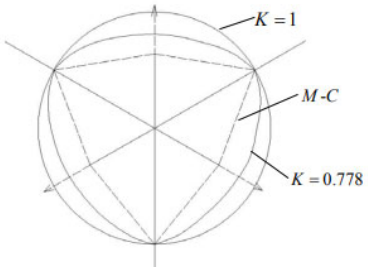

Figure 1-9. Different K values correspond to the yield surface of the rock on the plane

1.3. Evolution of rock damage

For continuous homogeneous dielectric materials, the stress-strain relationship expresses its main intrinsic properties. When the material exhibits softening characteristics under a certain load, the expression of material properties has high requirements for the quality of the model mesh, and the poor mesh quality will cause excessive energy dissipation and affect the accuracy of the calculation. ABAQUS software provides a variety of damage evolution methods, but no matter which one is used, the impact of the

model mesh on the computational accuracy should be avoided as much as possible. To solve this problem, the concept of feature length was introduced, which is represented as the unit size of the mesh in ABAQUS software, and is used to describe the relationship between material stress and displacement during the damage evolution phase. When damage occurs, the effective plastic displacement (u^{-pl}) is defined as the product of the characteristic length of the mesh (L) and the equivalent plastic strain (ε^{-pl}). In this case, the dissipation of energy during the destruction process is calculated in terms of unit area rather than unit volume. At the same time, energy is treated as an additional parameter of the material to calculate the amount of displacement in the event of complete failure, which is also in line with the definition of the critical energy release rate in the failure mechanism. In the ABAQUS software, two types of evolution based on effective plastic displacement and energy are provided, and this article will focus on three evolution methods based on effective plastic displacement.

(1) Tabular form:

Figure 1-11 shows that the damage evolution is defined in tabular form, that is, the specified equivalent plastic displacement and the corresponding damage ratio d are entered sequentially (when the damage ratio reaches 1, the material is considered to be damaged), which is flexible in data processing, and its function expression is as follows:

$$d = d(u^{-pl})$$

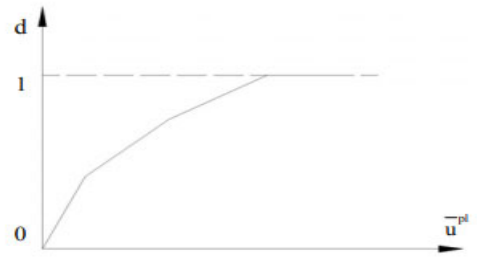

Figure 1-10. Evolution of material damage table based on equivalent plastic displacement

(2) Linear form:

In the process of damage evolution, the damage ratio and the equivalent plastic displacement form a linear growth trend, and the growth amplitude ratio is the same (i.e., the slope of the curve remains unchanged), which is suitable for the material damage evolution after passing the yield point, which shows a complete plastic response. The function expression is:

$$d = \frac{L\varepsilon^{pl}}{u_f^{-pl}}$$

(1) Exponential form:

After specifying the equivalent plastic displacement value of the material at the time of material failure, the curve approximation is used to express the evolution of the material damage, and when the index is taken to 0, it degenerates into a linear form. The expression of the function is shown in the following formula, and the selection of the index is based on the experimental data, and the equivalent plastic strain at the time of damage initiation and the plastic strain at failure are taken into account.

$$d = \frac{1 - e^{(u^{-pl}/u_f^{-pl})}}{1 - e^{-\alpha}}$$

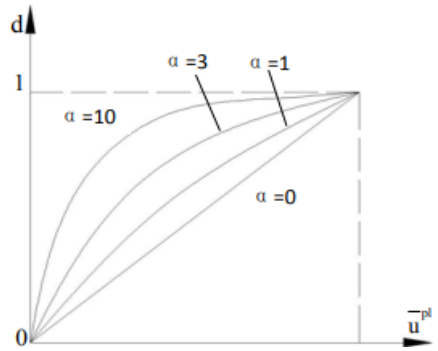

Figure 1-11. Linear evolution of material damage based on equivalent plastic displacement

In this simulation, the damage rules of rocks are in the form of tabular evolution, and the D-P criteria are used for rock failure

2. Single-tooth Rock Breaking Analysis

There are three main types of rock situations encountered by PDC teeth in the process of rock breaking: leveling rock, rock ridge, and rock ridge root. In addition, the PDC tooth now rotates around the center of the tool during the rock breaking process, and the rock model should be in the shape of a wellbore to reflect the real working conditions.

2.1. Establishment of finite element model

In this finite element simulation, the PDC scraping analysis was carried out under the conditions of rock ridge and flat rock, and the basic properties of the rock used are granite, as shown in Table 1-1.

Table 1-1. Rock parameters

Elastic modulus (GPa)	Poisson's ratio	Destruction displacement (mm)	Density (Kg/m^2)
58000	0.12	0.18	2.56

Figure 1-12 shows the geometric model of single-tooth scraping rock. The diameter of the cutting tooth is 10mm, the thickness is 10mm, and the cutting surface has a chamfer of 45 degrees and 1mm, and the main contents of this imitation Allah are shown in Table 1-2.

Table 1-2. Single-tooth scraping simulation content

Simulation type	Tooth diameter (mm)	Caster angle (°)	Roll angle (°)	Eat deep (mm)	Cutting speed (rad/s)
Flat rock cutting	10.00mm	15	0	2	8.37
Rock ridge root cutting	10.00mm	15	0	2	8.37
Ridge cutting	10.00mm	15	0	2	8.37

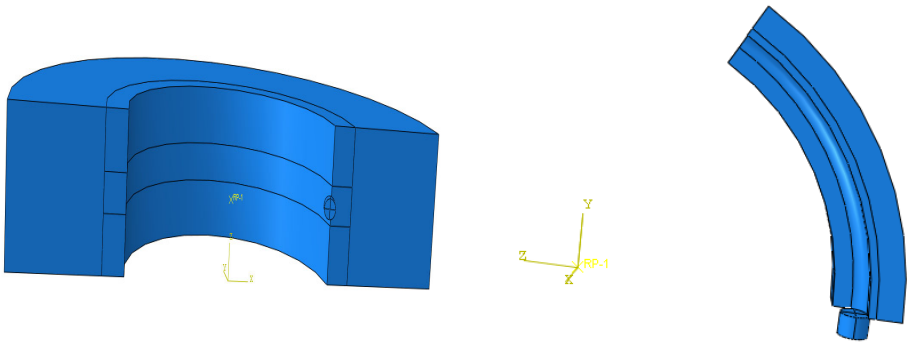

Figure 1-12. Single-tooth scraping model

2.2. Define contact and load conditions

Considering that the cutting surface is not in face-to-face contact with the rock during the PDC rock breaking process (there will be new rock contact with the PDC tooth after the failure of the contact rock), the PDC tooth is set as the main surface, the rock in the cutting area is set with a node set, the PDC cutting surface and the node set are set to surface-surface (explicit), and the contact attribute is set to the tangential behavior as the penalty function, the friction coefficient is set to 0.15, and the normal behavior is hard contact. The cutting tooth is coupled to the center point of the rock, a fixed constraint is applied to the rock, and the angular velocity is applied to the center point of the rock. The load application diagram is shown in 1-13.

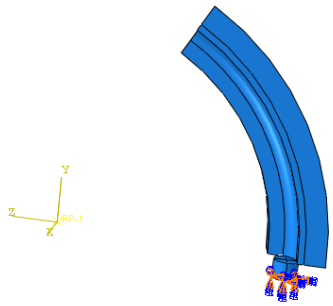

Figure 1-13. Single-tooth cutting load application

2.3. Analysis of single-tooth scraping simulation results

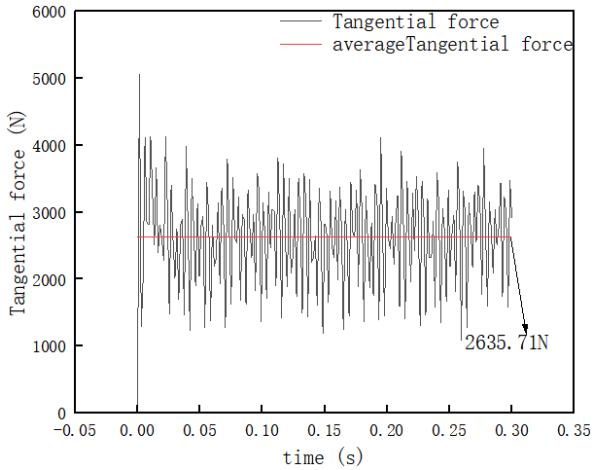

Figure 1-14. Tangential force-time relationship of planar rock

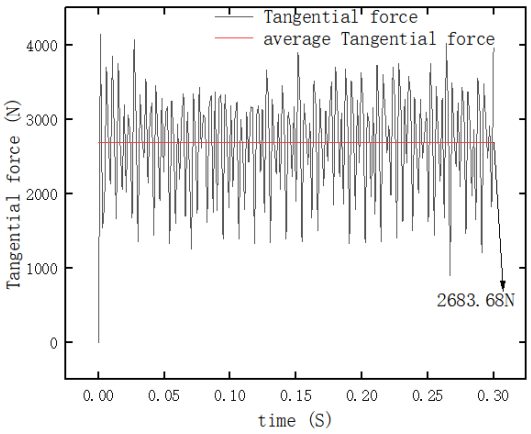

Figure 1-15. Tangential force-time relationship of rock ridge

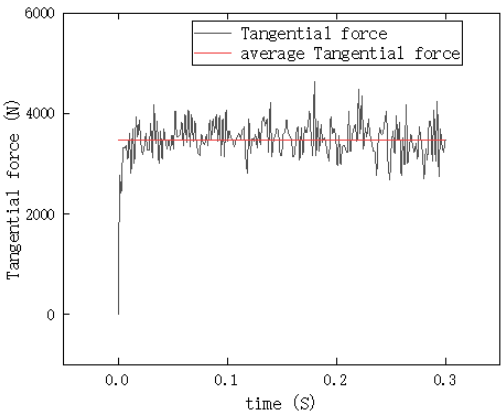

Figure 1-16. Tangential force-time relationship diagram of rock ridge root

Fig. 1-13, 1-14 and 1-15 are the relationship between the cutting force and time of the cutting teeth in the scraping plane rock, rock ridge and rock ridge root, respectively. It can be seen from the figure that the average tangential force of scraping on the plane rock is 2635.71N, the average average tangential force of scraping on the rock ridge is 2683.68N, and the average tangential force of the root of the scraping rock ridge is 3476.86N. Fig. 1-16 and Fig. 1-17 are the stress contours of the rock and rock ridge of the PDC tooth scraping plane respectively, it can be seen that under the action of load, the PDC tooth contacts with the rock and is broken, and the unbroken rock forms a new contact surface, so that the cutting trajectory is formed in reciprocation, and the crushing process of the rock is also accompanied by the change of the rock stress field, so the analysis of the stress field is helpful to analyze the crushing process of the rock and the rock breaking mode of the cutting tooth.

When the PDC tooth interacts with the rock, the tooth blade first contacts the rock and squeezes the rock, the stress peak occurs in the contact part between the rock and the tooth edge, and the rock near the tooth blade is extruded to cause plastic deformation and cracks, and the rock is shear damaged with the movement of the cutting tooth. The whole tooth surface begins to contact and extrude the rock, the stress on the rock section is evenly distributed in the part where the rock is in contact with the cutting tooth, under the extrusion of the cutting tooth, the pressure on the rock of the tooth surface part increases and pushes the surrounding rock, as the pressure exceeds the critical value of the rock is destroyed and removed from the rock mass, the rock section stress decreases.

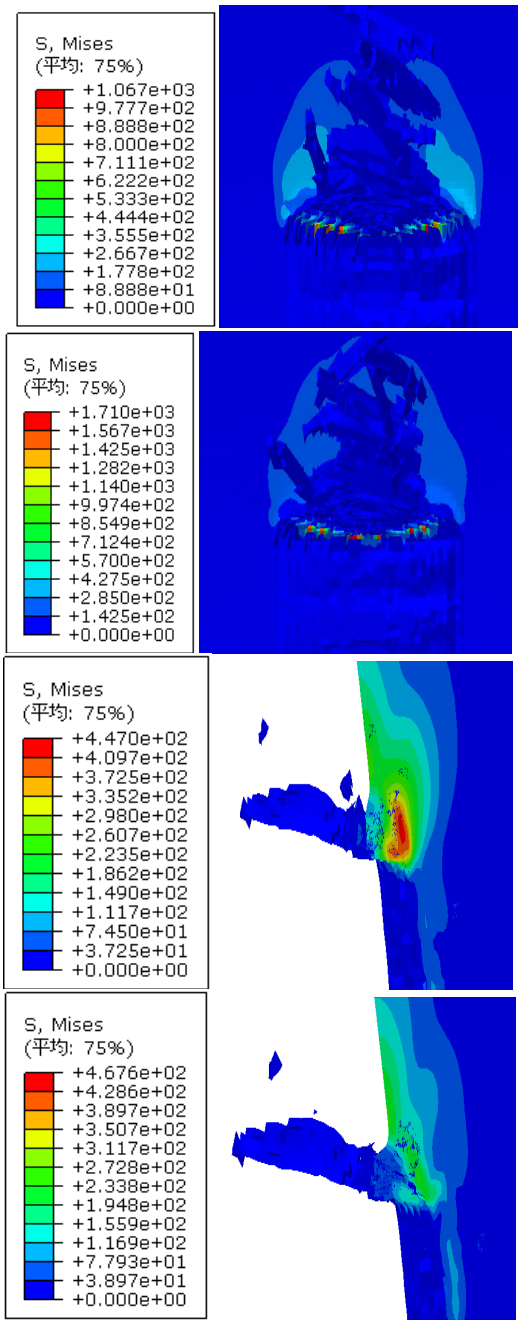

Figure 1-17. Stress contour of PDC tooth scraping and leveling rock

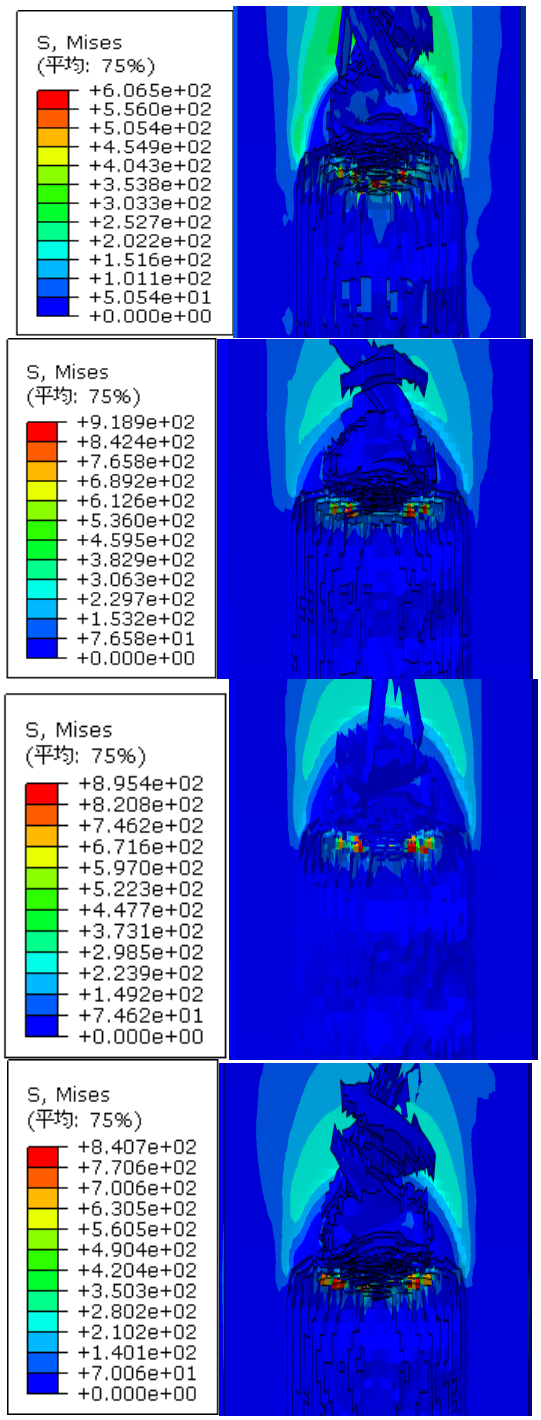

Figure 1-18. Stress contour of PDC tooth cutting rock ridge

From the analysis of Fig. 1-16 and 1-17, it can be seen that the stress range of the PDC tooth is greater than that of the flat rock scraping when the PDC tooth is scraped on the rock ridge. The larger the stress range, the more positive the crack generation of the rock, and at the same time is conducive to the propagation of the crack, which is equivalent to the pre-damage, which is conducive to rock crushing and improving the rock breaking efficiency.

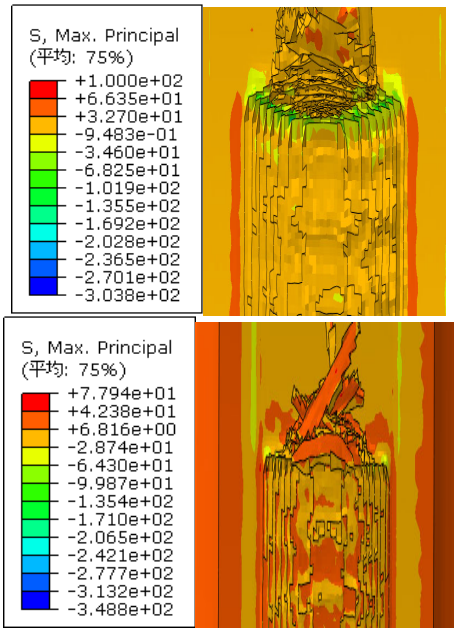

Figure 4-19. Maximum principal stress diagram of plane rock-ridge

As can be seen from Figure 1-18, the principal stress of the rock is distributed on both sides of the scraping trajectory when the PDC tooth scrapes the plane rock, and when scraping the rock ridge, the principal stress is not only located on both sides, but also produces an obvious stress concentration area, which is conducive to the crushing of the rock, thereby improving the rock breaking efficiency. As can be seen from Figure 4-18, the tensile strength of the rock is much smaller than the compressive strength of the rock, and the tensile stress generated during rock breaking also helps the rock to break.

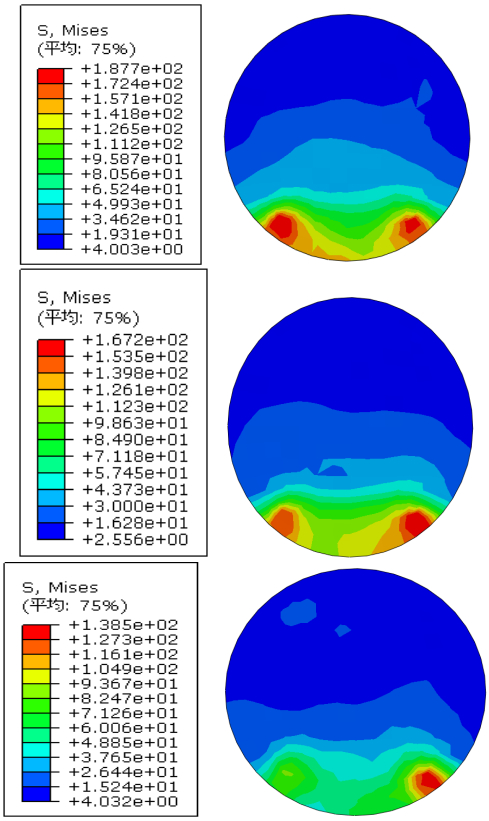

Figure 4-20. Instantaneous stress diagram of PDC tooth scraping rock ridge

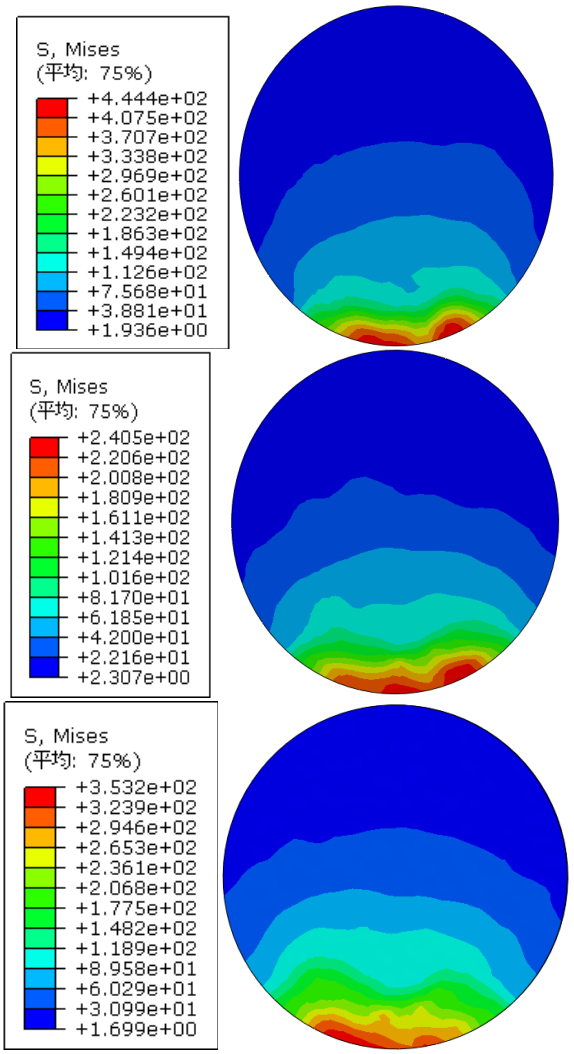

Figure 1-21. Instantaneous stress diagram of rock in the scraping plane of PDC teeth

From Figure 4-19 and Figure 4-20, it can be seen that the stress of the cutting tooth is mainly distributed in the area of interaction with the rock, and the maximum stress is distributed at the tooth edge of the tooth surface, and the stress at the distance from the tooth edge gradually decreases. As can be seen from Figure 4-19 and Figure 4-20, the stress of the PDC tooth when scraping the rock ridge is smaller than that of the scraping plane rock, which indicates that the PDC tooth blade bears less load when scraping the rock ridge.

3. The Influence of Different Factors on The Law of Rock Breaking of Cutting Teeth.

There are many parameters that affect the rock breaking of PDC tooth cutting, which are mainly divided into two types: structural parameters and working parameters. In this section, the structural parameters (PDC tooth diameter, tooth chamfer) and working parameters (camber angle, eating depth, scraping speed) are analyzed.

3.1. The influence of the diameter of the tooth on the rock breaking law of the cutting tooth

The density of the teeth of the reamer directly affects the arc length of the contact between the reamer and the rock, and affects the rock-breaking performance and life, the higher the

density of the teeth, the longer the life of the reamer, the larger the diameter of the teeth, and the lower the density of the teeth. In order to study the influence of tooth density on rock breaking performance, four cutting teeth with different diameters of 8mm, 10mm, 13.44mm, 16mm and 19mm were selected, and the rock breaking simulation was simulated at a 15° forward inclination angle, the cutting speed was 300mm/s, and the depth of 1.5mm was taken to simulate rock breaking. Both the tangential force and the axial force are increasing, and the specific work of crushing becomes smaller. It is because with the increase of the diameter of the cutting tooth, the area of the rock in contact increases, and the volume of the broken rock also increases, but the growth trend of the required cutting force is slowing down, so the specific work of crushing decreases. However, small diameter teeth can form large contact stresses in the contact area with the rock, and under the same conditions, small diameter teeth are more likely to destroy the rock than large diameter teeth.

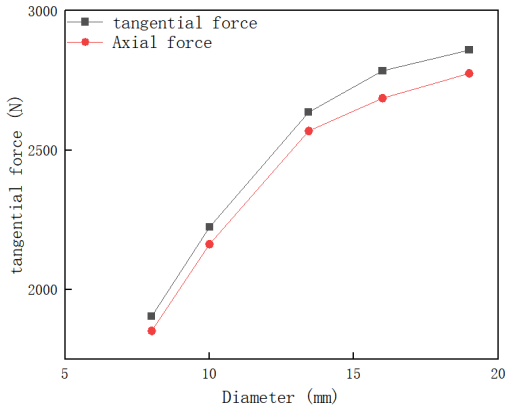

Figure 1-22. Tangential force and axial force change with diameter

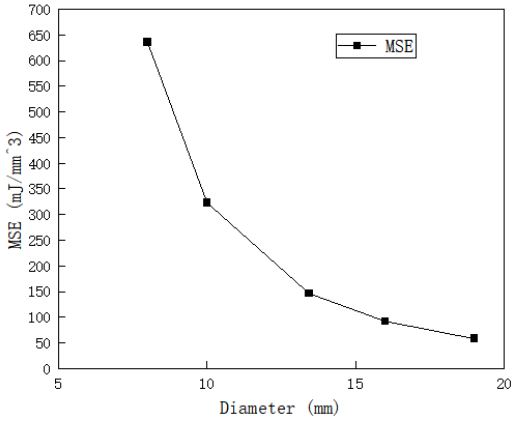

Figure 1-23. The specific work of crushing varies with diameter

3.2. Effect of chamfering

In order to explore its influence, the cutting teeth with a diameter of 13.44mm were taken, the chamfering angle was 45°, the length was 0.1mm, 0.2mm, 0.3mm, 0.4mm, 0.5mm, the cutting depth was 1.5mm, and the camber angle was 15°. The rock is albite. As can be seen from Fig. 4-23 and Fig. 4-24 below, with the increase of the chamfer angle of the PDC cutting teeth, both the tangential force and the axial force increase, and the increase of the axial force exceeds the increase of the tangential force. And both have the largest increase between 0.3mm and 0.4mm. After 0.1 mm to 0.2 mm, the axial force is greater than the tangential force. The crushing ratio increases with the increase of chamfer size, and it can be seen that the main factor affecting the crushing specific work is the tangential force.

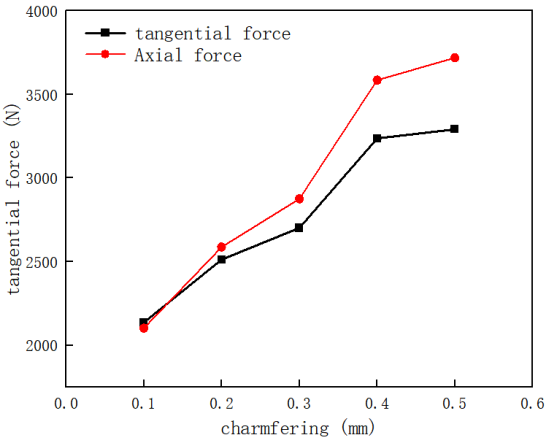

Figure 1-24. Tangential force and axial force vary with chamfer size

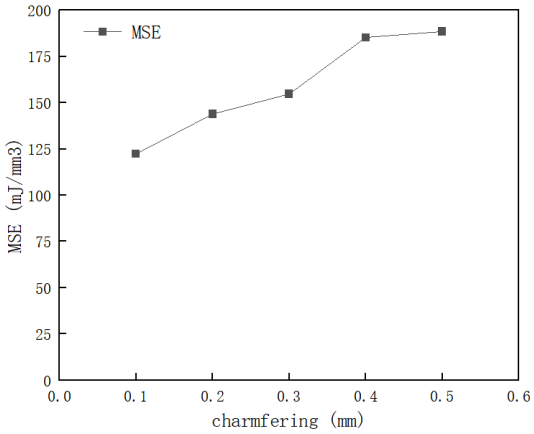

Figure 1-25. The specific work of crushing varies with the size of the chamfer

3.3. Effect of forward angle

The camber angle is one of the working parameters of the PDC cutting tooth, which has a significant impact on the rock breaking efficiency of the PDC tooth. The 13.44mm plane tooth was selected at a cutting depth of 1.5mm, with different camber angles (5°, 10°, 15°, 20°, 25°) for rock breaking simulation, and the variation law of tangential force, axial force and crushing specific energy obtained by the simulation data with the forward tilt angle of the cutting tooth is shown in Figure 4-23 and Figure 4-24, from which it can be seen that with the increase of the forward tilt angle, the axial force and tangential force are increasing, and when the forward angle is 5°, the axial force and tangential force are the smallest. And the difference is also the smallest of the five sets of data. At the same time, the influence of the forward tilt angle on the crushing specific work also increases with the increase of the forward tilt angle, but the crushing work ratio increases linearly. The increase of the dip angle will cause the cutting teeth to have a compressive effect on the rock. Due to the extrusion action, it is not conducive to rock breaking. It will increase the tangential force, axial force and crushing power ratio. For flat teeth, a suitable rake angle should be selected to avoid this phenomenon.

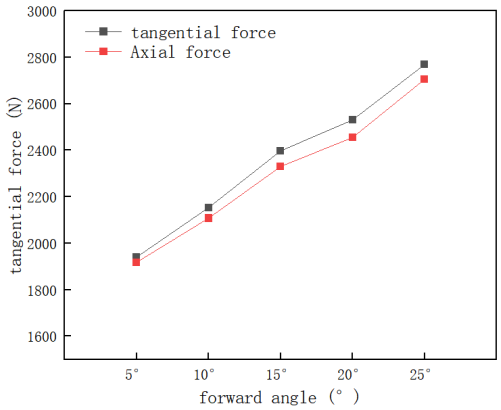

Figure 1-26. Tangential force-axial force varies with the camber angle

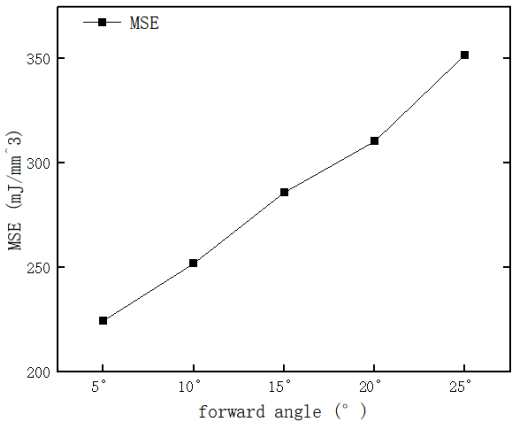

Figure 1-27. The crushing common ratio varies with the forward tilt angle

3.4. Effect of cutting speed

In order to study the influence of cutting speed on rock breaking, the cutting speed is set to 400mm/s, 500mm/s, 600mm/s, 700mm/s, 800mm/s, the cutting depth is 1.5mm, the caster angle is 15°, the cutting simulation time is 0.05s, and the diameter of the cutting teeth is 13.44mm. Fig. 4-24 and Fig. 4-25 are the variation of axial force and tangential force with cutting speed and the crushing power ratio with cutting speed, respectively. It can be seen from Figure 4-24 that with the increase of cutting speed, the axial force and tangential force of PDC cutting teeth are increasing, and it can be seen from Figure 4-25 that the crushing work ratio increases with the increase of cutting speed, but the increase amplitude is significantly reduced.

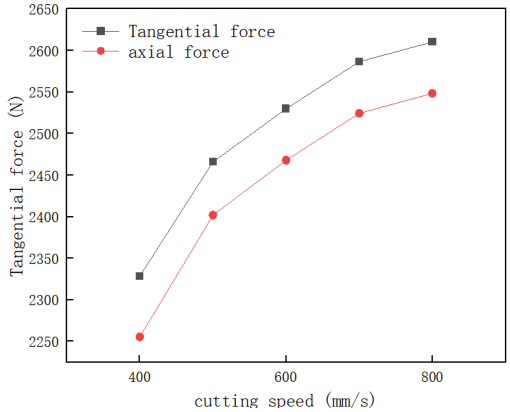

Figure 1-28. Effect of cutting speed on tangential and axial forces

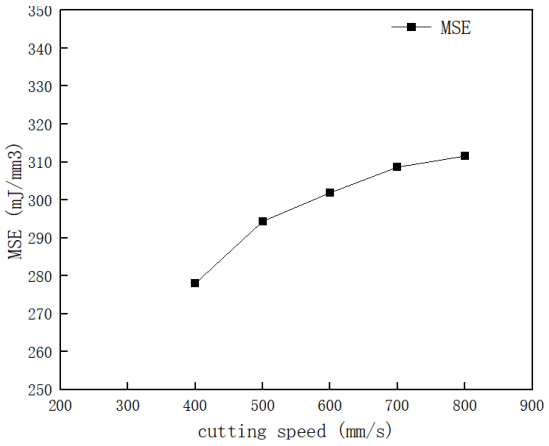

Figure 1-29. Effect of cutting speed on crushing ratio

3.5. Effect of depth of cut

The cutting depth is a very important parameter for rock cutting, which affects the crushing mode of the rock, the crushing mode of the rock is changed by different cutting depths, the cutting tooth with a diameter of 13.44mm is selected, and the rock breaking simulation is carried out at a forward inclination angle of 15° and different feeding depths (2mm, 2.5mm, 3mm, 3.5mm, 4mm), and the tangential force, axial force and crushing power ratio of the PDC tooth are processed to obtain the variation law of the PDC tooth with the depth of ingress as shown in Figure 4-26 and Figure 1-30. It can be seen from Fig. 1-30 and Fig. 1-31 that the tangential force and axial force increase with the increase of the depth of intake, and the ratio of crushing work decreases with the increase of the depth of intake.

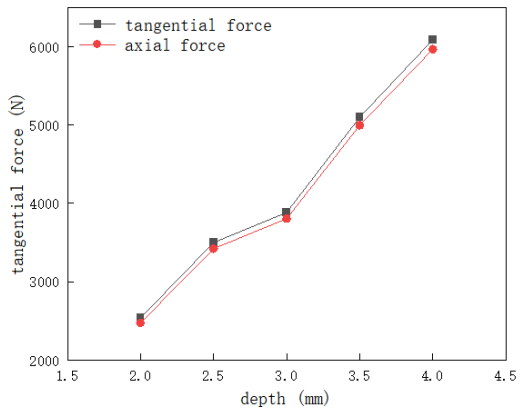

Figure 1-30. Variation of intake depth with tangential force and axial force

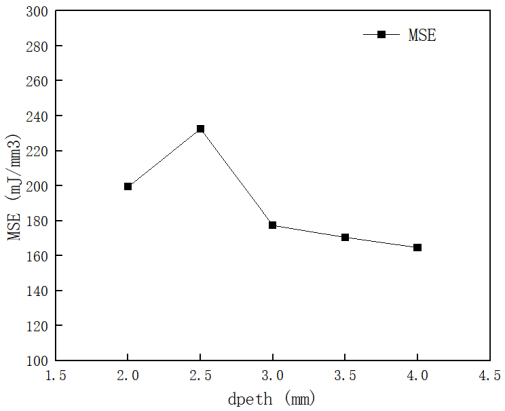

Figure 1-31. Effect of ingestion depth on crushing power ratio

4. Conclusion

In this chapter, the PDC cutting teeth are analyzed based on the finite element simulation method, and the stresses of the PDC teeth in the scraping plane rock, rock ridge and rock ridge root and rock stress are analyzed, and the influence on tangential force, axial force and crushing power ratio is analyzed from five factors: tooth diameter, tooth chamfer size, forward tilt angle, cutting speed and crushing depth. The following conclusions can be drawn:

(1) When the PDC tooth is scraped and cut on the rock ridge, the stress range of the rock ridge is greater than that of the flat rock. It is conducive to the crushing of rock, when the PDC tooth scrapes the plane rock, the principal stress of the rock is distributed on both sides of the scraping trajectory, and when scraping the rock ridge, the principal stress is not only located on both sides, but also produces an obvious stress concentration area, which is conducive to the crushing of the rock.

(2) From the perspective of the stress of the PDC tooth surface, when scraping the plane rock, the stress is mainly located in the contact area between the PDC tooth surface and the rock, and the stress gradually decreases away from the contact area, and the stress is concentrated in the tooth edge, which is known from the second chapter, which will cause the cemented carbide base to produce stress bands. When scraping the rock ridge, the stress of the PDC tooth is concentrated on both sides, and the stress is less than that of the cutting plane rock.

(3) The axial force and tangential force of the PDC cutting tooth increase with the increase of the diameter of the tooth, and the crushing work ratio decreases with the increase of the diameter. With the increase of the size of the chamfer, the axial force and tangential force also increase, and the crushing power ratio also increases. The axial force, tangential force and crushing work ratio of the cutting tooth increase with the increase of the cutting raking angle. With the increase of cutting speed, the axial force and tangential force of the cutting tooth are also increasing, but the increasing trend is decreasing, and the crushing power ratio is also the same trend. With the increase of the depth of intake, the tangential force and axial force of the cutting teeth increase linearly, and the crushing work ratio increases first and then decreases.

References

[1] Cai Meifeng. Rock mechanics and engineering[M]. Science Press,2007:219-228.

[2] Yu Maohong. The development of the 20th century rock strength theory – commemorating the 100th week of the development of the Mohr-Coulomb strength theory Year[J]. Chinese Journal of Rock Mechanics and Engineering. 2000, 19(5): 545 – 550.

[3] Andreev G. Brittle Failure of Rock Materials: Test Results and Constitutive Models [M]. Rotterdam: A. A. Balkema，1995.

[4] Sheorery P R. Empirical Rock Failure Criteria [M].Rotterdam: A. A. Balkema, 1997.

[5] Fei Kang. Application of ABAQUS in geotechnical engineering[M]. China Water Resources and Hydropower Press, 2010:67-77.